Geomorphology xxx (2017) xxx–xxx

Contents lists available at ScienceDirect

Geomorphology

journal homepage: www.elsevier.com/locate/geomorph

The influence of channel bed disturbance on benthic Chlorophyll *a*: A high resolution perspective

Scott B. Katz [a,b], Catalina Segura [a,b,*], Dana R. Warren [c,d]

[a] Forest Engineering, Resources, and Management, Oregon State University, 201 Peavy Hall, Corvallis, OR 97331, USA
[b] Water Resources Graduate Program, Oregon State University, 116 Gilmore Hall, Corvallis, OR 97331, USA
[c] Department of Forest Ecosystems and Society, Oregon State University, Corvallis, OR 97331, USA
[d] Department of Fisheries and Wildlife, Oregon State University, Corvallis, OR 97331, USA

ARTICLE INFO

Article history:
Received 17 May 2017
Received in revised form 13 November 2017
Accepted 13 November 2017
Available online xxxx

Keywords:
Disturbance
Resilience-resistance
Periphyton
Mountain stream

ABSTRACT

This study explores how spatial dynamics and frequency of bed mobility events in a headwater stream affect the spatial and temporal variability in stream benthic algal abundance and ultimately the resilience of benthic algae to stream scouring events of different magnitudes. We characterized spatial variability in sediment transport for nine separate flow events (0.1–1.7 of bankfull flow), coupling high resolution (<0.1 m^2) two-dimensional shear stress values with detailed measurements of the channel substrate. The stream bed was categorized into regions of high and low disturbance based on potential mobility of different grain sizes. High resolution (<0.25 m^2), in situ measurements of benthic Chlorophyll-*a* concentrations (Chl-*a*) were taken on 18 sampling dates before and after high flow events in regions of the streambed with contrasting disturbance to understand how benthic algal communities respond to sediment transport disturbance through space and time. According to the modeling results, the percentage of the channel likely to be disturbed varied greatly across the different flows and considered grain sizes between 7.7 and 70.4% for the lowest and highest flow events respectively. Mean shear stress in the channel bed across all sampling dates explained 49% of the variance in Chl-*a*. Over the 18 sampling dates — encompassing post-disturbance impacts and subsequent recovery — Chl-*a* differed between disturbance level categories defined based on the relative movement of the median grain size on 14 occasions. However, low disturbance locations were not always associated with higher Chl-*a*. The algal Chl-*a* biomass at any given time was a function of the stage of algal recovery following a high flow event and the magnitude of the disturbance itself — impacting algal loss during the event. Resistance of the algal communities to bed disturbance and resilience to recovery following a flow event varied spatially. Areas with low shear stress were less susceptible to scour during moderate disturbance events but were slower to recover when scour occurred. In contrast, high shear stress areas responded rapidly to flood events with rapid declines, but also recovered more quickly and appeared to have high potential for maximum accrual within our study reach. Ultimately, timing along with the inverse relationship between resiliency and disturbance frequency highlights the complexity of these processes and the importance of studying the interactions between geomorphic and ecological processes with high resolution across spatial and temporal scales.

1. Introduction

The process of sediment transport and deposition is a fundamental organizing feature in fluvial systems that sets the physical habitat template of stream environments. Indeed, bed mobility is widely recognized as a key organizing feature for ecosystem processes and biota in streams (Peckarsky et al., 2014). Bed mobility and substrate scour that occurs during sediment transport and deposition are particularly important abiotic processes for stream primary production because they have the potential to remove benthic algae and reset the succession of stream periphyton communities (Fisher et al., 1982; Biggs et al., 1999). Given the role of instream primary production in supporting aquatic biota and controlling stream nutrient dynamic, the resilience of stream primary producers — their capacity to withstand and recover from disturbance events (Holling, 1973; Bone et al., 2016) — is an important stream characteristic.

In systems with low substrate stability throughout a reach and during large discharge events when nearly all of the bed is mobile, abrasion caused by small particles combined with the molar movement of large particles scrapes away most of the existing benthic algae (Dodds et al., 1996; Rosenfeld and Hudson, 1997; Uehlinger, 2000; Uehlinger et al., 2003; Uehlinger, 2006; Hoellein et al., 2007; Atkinson et al., 2008;

* Corresponding author at: Forest Engineering, Resources, and Management, Oregon State University, 201 Peavy Hall, Corvallis, OR 97331, USA.
E-mail address: segurac@oregonstate.edu (C. Segura).

https://doi.org/10.1016/j.geomorph.2017.11.010
0169-555X/

Holtgrieve et al., 2010; Luce et al., 2010; Segura et al., 2011; Gerull et al., 2012). For these large events that fully reset the system in regard to benthic algal communities, an assessment of resilience necessarily focuses the recovery of streambed algal standing stocks to pre-event levels (i.e., engineering resilience). In this context, recovery rates are key to understanding the temporal dynamics of stream primary production as well as nutrient demand and food resources for secondary production. During more moderate discharge events or when considering ecosystem processes over time scales that encompass low-flow conditions, considering stream resilience as a combination of recovery and the potential to maintain ecosystem function (i.e., ecological resilience) may be more appropriate (Holling, 1973; Hodgson et al., 2015; Bone et al., 2016). In this study, we use a two-dimensional hydraulic model to estimate stream bed mobility and repeated high resolution assessments of stream benthic algal standing stocks in a western Oregon stream to assess potential ecological and engineering resilience of stream primary producers to moderate and large extent sediment transport events.

High flow disturbances can remove benthic algae through (i) dislodging or breaking algae from its hold on a substrate through the elevated shear stress caused by increased water velocity, (ii) abrasion by mobilized sediments that scours and breaks algae off from its substrate, and (iii) molar action of tumbling gravel/cobble substrata upon which algae grow that scrapes the algae from substrates (Francoeur and Biggs, 2006). Although the importance of these processes has been recognized for decades in a broad sense (Resh et al., 1988; Reice et al., 1990; Biggs et al., 1999; Hart et al., 2013) most work quantifying mobility of the bed in relation to primary production and algal biomass has represented the flow field in one dimension. That is, assuming that the distribution of the flow field is uniform or that substrate mobilizes homogeneously across entire reaches or cross sections. This one-dimensional perspective misses for instance the potential to identify low mobility sections of a stream where scour may be more limited thereby allowing for persistence of benthic primary producers (Pitlick and Wilcock, 2013). We lack a clear conceptual framework that considers bed mobility events on two dimensions — with associated effects on stream ecosystem resilience. Part of the difficulty in developing this framework lies in the fact that benthic periphyton removal processes (i–iii above) are temporally and spatially variable. For example, while changes in sediment supply often vary at the basin or subbasin scale, discharge and channel morphology often vary at the reach scale; and shear stress and grain size distributions (GSD) in the channel bed vary at the patch scale. Considering the patch scale in particular, at this spatial resolution, different locations in the stream may undergo contrasting geomorphic processes simultaneously during a high flow event where active movement of bed material may occur in one spot while other spots are completely stable (Segura and Pitlick, 2015). This leads to spatially variable responses of benthic communities to increasing discharge within a reach (Biggs and Stokseth, 1996; Uehlinger et al., 2003). Early studies that evaluated the magnitude of scouring disturbance to benthic algal communities were based on peak discharge (Fisher et al., 1982; Biggs and Close, 1989; Segura et al., 2011; Townsend and Douglas, 2014) or one-dimensional models of sediment transport (Uehlinger et al., 1996; Biggs et al., 1999). These studies therefore overlook the potential for spatial changes in transport intensity during an individual event (Lisle et al., 2000; Stewart et al., 2005; May et al., 2009; McDonald et al., 2010; Legleiter et al., 2011; Segura et al., 2011; Segura and Pitlick, 2015), which could contribute to other factors that create spatial variability in benthic algae on the stream benthos (Stevenson, 1990; Jowett and Biggs, 1997; Biggs et al., 1999; Francoeur and Biggs, 2006; Townsend and Douglas, 2014). Algal abundances can vary at different spatial and temporal scales because of differences in scour, grazing pressure, light availability, and nutrient concentrations in the surrounding water. Variability in algal biomass can manifest at local scales across an individual sediment particle (Sekar et al., 1999; Kanavillil et al., 2015), at the patch scale among different sediment particles (Cattaneo et al., 1997), at the habitat unit scale of the stream bed associated with different morphologies such as riffles and pools (Cardinale et al., 2002; Segura et al., 2011; Luce et al., 2013), and broadly across stream reaches and among streams (Bernot et al., 2010). Patchiness in algal biomass prior to a disturbance and patchiness in bed mobility and scouring processes within a reach together will affect the amount of biomass lost during high flow events; and the magnitude of biomass reduction caused by an individual high flow in turn influences how the community will recover after the disturbance has occurred (Biggs and Close, 1989; Peterson et al., 1994; Biggs et al., 1998; Snell et al., 2014; Coundoul et al., 2015). However, capturing the background heterogeneity in Chlorophyll *a* (Chl-*a*) abundance and deciphering the influence of variable scour from other factors that affect spatial variability in benthic algal standing stocks is challenging. Common sampling protocols assess few (i.e., <30) sediment particles that are selected at random through a reach (Biggs and Close, 1989; Davie and Mitrovic, 2014; Townsend and Douglas, 2014), at transects across a reach (Biggs et al., 1999; Townsend and Padovan, 2005), at patches (Segura et al., 2011), or in other systematic sampling schemes. In the few studies to date where spatial variability in sediment transport disturbance to benthic algae has been investigated, the experiments were conducted in streams with snowmelt flow regimes that experienced only one large mobilization event per year that fully reset the system. This limited the possibility to investigate the response and recovery of benthic algae to multiple disturbance events of different magnitudes (Segura et al., 2011). In this study, we use a novel Chl-*a* assessment method that allows for frequent in situ estimates of benthic algal standing stocks to overcome issues of spatial and temporal resolution in quantifying the response of benthic algae to multiple high flow events in a rain-dominated system.

The objective of this study was to evaluate resilience of stream benthic algal abundance to high flow events. We consider the spatial dynamics of disturbance and the potential for low shear stress areas to provide refuge habitat for benthic algae and the recovery of benthic algae following moderate and high flow disturbance events. We apply a two-dimensional (2D) shear stress model that encompasses a wide range of flows ($0.2Q_{bf}$ to $>Q_{bf}$) to determine the influence of sediment mobility on scour across the streambed and to assess recovery of benthic Chl-*a* at high spatial resolution (<0.25 m^2) that can encompass areas with low and high shear stress. Understanding how the magnitude of high flow and bed scouring event disturbances affect primary production across two dimensions is important for a wide range of environmental management applications including setting meaningful environmental flow targets (Osmundson et al., 2002; Davie and Mitrovic, 2014), restoring natural processes through river rehabilitation projects (Murdock et al., 2004; Lake et al., 2007; Stanley et al., 2010), or quantifying river metabolic and production rates relevant to higher tropic levels.

2. Study site and methods

2.1. Study site

This study was conducted in a cobble-gravel bed reach of Oak Creek, Oregon (Fig. 1). The forested catchment drains 7 km^2 underlain by basaltic lithology (Milhous, 1973; O'Connor et al., 2014) in a region with Mediterranean climate characterized by wet winters and cool/mild summers. The study reach has a pool-riffle sequence in the upstream end and a relatively straight section in the downstream section. The reach is located directly upstream from a historic sediment transport sampling facility where bedload samples were collected between 1969 and 1973 (Milhous, 1973) and which currently provides a square cement weir where an accurate discharge to stage height relationship can be built. The bankfull dimensions of the study reach channel are 6 m in width and 0.46 m in depth. The reach average slope is 0.014 m/m, and the bankfull discharge (Q_{bf}) is 3.4 m^3/s (Milhous, 1973). Elevations within the basin range from 143 to 664 m (Paustian and Beschta, 1979). The basin is located in the McDonald-Dunn Forest,

Please cite this article as: Katz, S.B., et al., The influence of channel bed disturbance on benthic Chlorophyll *a*: A high resolution perspective, Geomorphology (2017), https://doi.org/10.1016/j.geomorph.2017.11.010

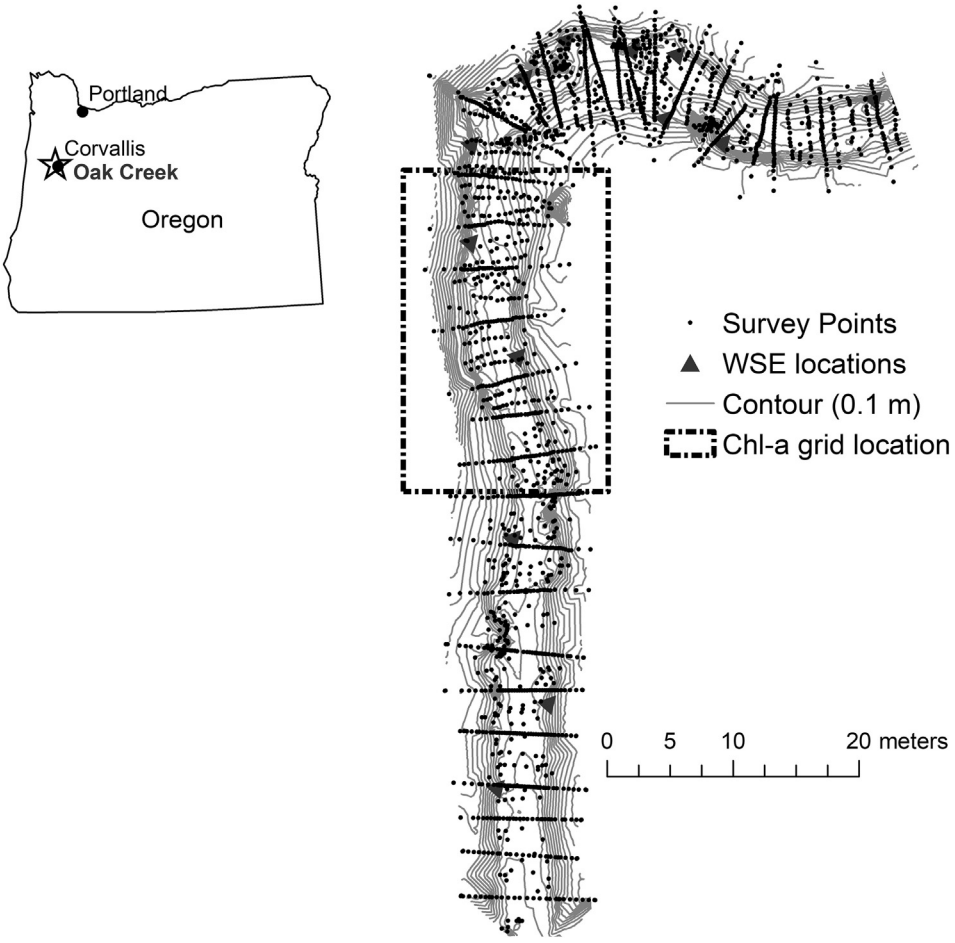

Fig. 1. Location of the study reach in Oak Creek, OR. Topographic surveying points, derived 0.1-m contours, water surface elevation (WSE) monitoring locations, and the location of the grid used to monitor Chlorophyll *a* are also included.

which is owned and managed by the College of Forestry at Oregon State University and dominated by Douglas fir (*Pseudotsuga menziesii*) and Oregon White Oak (*Quercu* sp). In the riparian area surrounding the study site the dominant species include Alder *(Alnus* sp), Black Cottonwood (*Papulus trichocarpa*), and Big Leaf Maple (*Acer macrophyllus*) with lower densities of fir and oak.

2.2. Characterization of channel topography, grain size, and discharge

Detailed measurements of channel geometry and grain size were collected in the study reach in the summer of 2015. Over 2000 bed elevation points were surveyed with a total station during this period (Fig. 1). The survey included 32 cross sections (XS). Cross sections were established every 3 m (half bankfull width apart) with additional survey points added between them to capture slope breaks such as riffle crests, the channel thalweg, and the toe and top of banks. This topographic information was interpolated across the area of the reach (Merwade et al., 2008; Merwade, 2009) and the interpolated map was used as an input to the 2D hydraulic model (see below). Bed surface grain size distribution (GSD) was characterized with 23, 100-particle pebble counts along surveyed cross sections (Wolman, 1954). Grain size fractions for the 16th, 50 th, and 84 th percentile were 19 ± 1.1, 45.1 ± 2.5, and 83.2 ± 3.5 mm respectively (Katz, 2016). The reach hydrograph was calculated based on a rating curve coupled with water elevation measurements taken at the downstream end of the reach using a Hobo U20 Water Level logger (Fig. 2). The rating curve covered discharge values up to 3.9 m^3/s ($1.1Q_{bf}$). Flows were above this value during one event for 18 h during the study period (Fig. 2).

2.3. Hydraulic model

We estimated mean velocity (U) and shear stress (τ) for seven flows (0.4–3.4 m^3/s, $0.12Q_{bf}$ - Q_{bf}) using the Flow and Sediment Transport with Morphological Evolution of Channels (FaSTMECH) analytical solver (McDonald et al., 2006). The model uses a finite difference solution to the Reynolds-averaged momentum equations (Nelson et al., 2003). The calculations are performed within an orthogonal curvilinear grid that follows the surveyed planform topography of the channel (Nelson and Smith, 1989) and divides local velocities into cross-stream and downstream components (v and u respectively). The model inputs include bed topography, discharge (Q), roughness (estimated with a constant or variable drag coefficient, C_d), a measure of lateral eddy viscosity (LEV), and the downstream stage. The model calibration procedure involves adjusting the C_d and LEV to minimize the root mean square error (RMSE) between modeled and observed water surface elevation (WSE) at 13 locations (Fig. 1). Shear stress is calculated in the model based on velocity, water density (ρ), and the drag coefficient:

$$\tau = \rho C_d (u^2 + v^2) \quad (1)$$

Model calculations were conducted for the entire reach using a 0.2-m grid to ensure a flow domain long enough for the model to achieve a robust calibration and to ensure no influence on the sampling grid by

Please cite this article as: Katz, S.B., et al., The influence of channel bed disturbance on benthic Chlorophyll *a*: A high resolution perspective, Geomorphology (2017), https://doi.org/10.1016/j.geomorph.2017.11.010

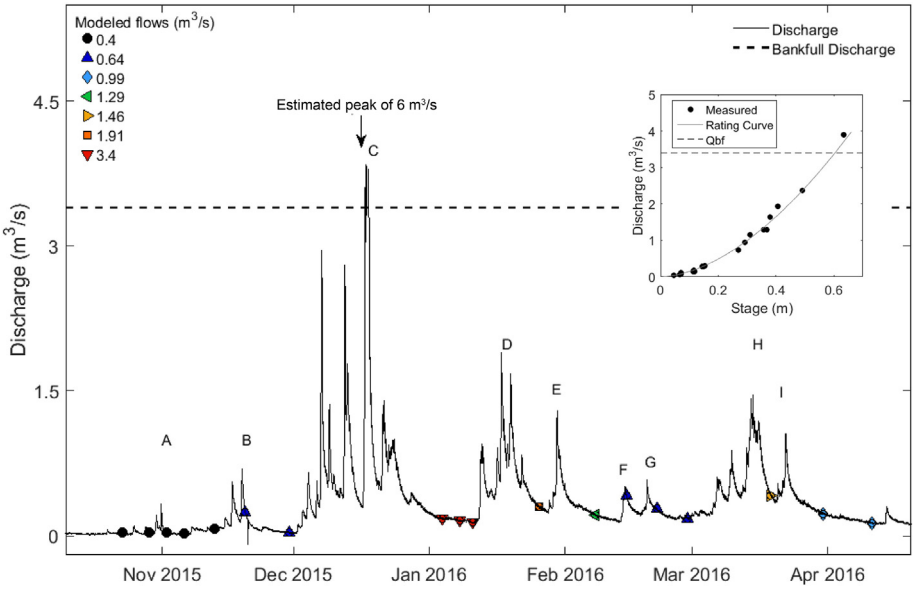

Fig. 2. Hydrograph of Oak Creek, OR, during study period. Discharge values are calculated based on measurements taken at 10-min intervals and on the site-rating curve (see insert). Chlorophyll-*a* sampling events are indicated with the markers color coded according to the flow event used to describe shear stress conditions for the preceding high flow events (A–H).

the boundary conditions. We collected Chl-*a* in a smaller section of the reach (see Section 2.4). The number of wetted grid nodes in the model domain varied from 9031 to 14,951 depending on flow level (Table 1). A constant C_d was used for each model run. The RMSE between predicted and measured WSE varied between 0.025 and 0.048 m and the $R^2 >$ 0.994. Calibrated C_d and LEV ranged from 0.017 to 0.04 and from 0.0010 to 0.0032 respectively. The WSE RMSE were well within acceptable ranges found in other studies using FaSTMECH.

2.4. Characterization of benthic Chlorophyll a

We measured the concentration of benthic photosynthetic pigments using a BBE Moldaenke BenthoTorch (http://www.bbe-moldaenke.de). The Benthotorch is a hand held, in situ fluorimeter that estimates Chl-*a* directly from the stream substrate based on absorbance of fluorescent light (Kahlert and McKie, 2014). We used the benthotorch values as a surrogate for Chl-*a* concentration as it is the dominant pigment measured by this device and because Chl-*a* is the dominant photosynthetic pigment the benthic algae of this and other streams across the coast range (Gregory, 1980). Further, benthic Chl-*a* concentrations are correlated with instream primary production in headwater streams (Roberts et al., 2007; Bernot et al., 2010), which allows us to relate algal standing stocks to stream ecosystem function (primary production) in considering ecological resilience in this system. We use the term Chl-*a* hereafter to refer to benthotorch values for Chl-*a* concentrations. The Chl-*a* measurements were taken on 18 separate occasions before and after high flow events between 23 October 2015 and 11 April 2016 (Fig. 2). The Chl-*a* measurements were made within a 20-m section of the reach (Fig. 1) using a gridded sampling scheme. The grid had a spacing of 0.5 m × 0.5 m and a total of 352 cells. Five replicates were randomly selected within each (0.25 m^2) grid cell; however, we avoided sampling the same area twice within a sampling period. Grid cells were only sampled when the entire grid cell was submerged and the stream substrate within the cell was visible (i.e., no leaves). In order to minimize disturbance of the stream substrate in sampled cells, measurements were taken across alternating rows moving from downstream up. The area of the grid is surrounded primarily by deciduous vegetation with relatively similar light availability (i.e., similar shading from the riparian area). Direct sunlight on the stream reach was limited during most sampling events.

Table 1
FaSTMECH model development and calibration summary: discharge (Q_i), ratio of Q_i to bankfull flow (Q_i/Q_{bf}), downstream (D.S.) stage, the number of calculation nodes, the root mean square error (RMSE) between measured and modeled water surface elevations (WSE), the coefficient of determination (R^2) of the relation between measured and modeled WSE, the calibrated drag coefficient (C_d), and lateral eddy viscosity (LEV)

Q_i	Q_i/Q_{bf}	D.S. stage[a]	# wet nodes	RMSE (m)	R^2	C_d	LEV
0.4	0.12	98.91	9031	0.048	0.994	0.040	0.001
0.64	0.19	98.96	9830	0.028	0.996	0.0380	0.0016
0.99	0.29	99.03	10,393	0.031	0.996	0.0250	0.0024
1.33	0.39	88.08	10,840	0.028	0.997	0.0180	0.0032
1.46	0.43	99.10	11,036	0.025	0.997	0.0170	0.0031
1.91	0.56	99.17	11,905	NA[b]	NA[b]	0.0210	0.0025
3.41	1.00	99.34	14,951	0.031	0.996	0.0350	0.0010

[a] From an arbitrary datum
[b] N/A: Not available, the flow was calibrated based on the relationship between calibrated C_d and Q for the other flow scenarios and not based on WSE.

2.5. Stream abiotic factors: nutrients, light, and temperature

Water samples were collected monthly during the study period for analysis of nitrate (NO_3^--N), ammonia (NH_4^+-N), and phosphate (PO_4^{3-}-P). The samples were analyzed for nitrate and phosphate using a Dionex ICS-1500 ion chromatograph. The ammonia analysis was performed using a Technicon Auto-Analyzer II. Light was measured using a HOBO pendant light sensor and an Odyssey photosynthetically active radiation (PAR) logger. The sensors were suspended above the stream bed within the middle of the sampling grid at the edge of the bank. The light intensity meter was deployed from 23 October 2015 to 16 November 2015 and again from 8 January 2016 to 19 March 2016. The PAR sensor was deployed between 8 February 2016 and 11 April 2016. A relationship was developed between LUX and PAR in order to convert the light intensity data to PAR for the entire study period. Stream temperature was measured at 10-min increments in two locations: downstream with the Hobo U20 water level logger (precision of ±0.44 °C) and upstream with a Solinst Edge water level logger (±0.05 °C) located 30 m upstream from the reach.

Please cite this article as: Katz, S.B., et al., The influence of channel bed disturbance on benthic Chlorophyll *a*: A high resolution perspective, Geomorphology (2017), https://doi.org/10.1016/j.geomorph.2017.11.010

2.6. Disturbance characterization

Channel bed disturbance was characterized using the model estimates of shear stress coupled with the D_2 (7 mm), D_{50} (45 mm), and D_{84} (83 mm) to assess the likelihood of channel bed disturbance via the Shield's stress:

$$\tau^* = \frac{\tau}{(\rho_s - \rho)gD_i} \quad (2)$$

where τ_i^* is the Shield's stress associated with the movement of given grain size (D_i), ρ is the density of water (1000 kg/m^3), and ρ_s is the density of the sediment (2850 kg/m^3 for basalt). We used a hiding function to estimate the reference shears stress for motion for each D_i (τ_{ri}^*) based on reference measured value for D_{50} for Oak Creek, $\tau_{r50}^* = 0.040$ (Parker, 1990):

$$\frac{\tau_{ri}^*}{\tau_{r50}^*} = \left(\frac{D_i}{D_{50}}\right)^{-\gamma} \quad (3)$$

We assumed a γ value of 0.8. This information was used to calculate the percentage of the channel bed in which the movement of each size fraction was possible and to explore the relation between abrasion (i.e., movement of smaller fractions) and saltation of larger particles and the observed concentrations of benthic Chl-*a*. In order to look at the influence of disturbance on the temporal variability of Chl-*a*, we assigned a disturbance category to each grid that changed depending on the flow level and shear stress distribution. The high disturbance category was assigned to grid cells when $\tau_i^*/\tau_r^* \geq 1$ and to the low disturbance category when $\tau_i^*/\tau_{ri}^* \leq 1$. These values correspond to regions of the streambed where mobilization of the D_2, D_{50}, or D_{84} are expected to either occur (high) or not occur (low).

The shear stress values for each high flow event (A–I) were defined based on the modeled results from the flow closest in magnitude to each instance (Table 2). The results from these modeled high flow events were then used to define the flow conditions and channel bed disturbance for the subsequent Chl-*a* sampling events (see color markers in Fig. 2). In doing so, we are investigating the effect that recent high flow events of different magnitudes and the movement of different size fractions have on Chl-*a* loss and growth dynamics (Table 2 and Fig. 2).

3. Results

3.1. Flow regime

The flow regime for Oak Creek during the study period was typical of a rainfall-dominated system with frequent high flow events during the wet season. Oak Creek experienced a series of nine high flow events (A–I) between 23 October 2015 and 11 April 20,146 that ranged in peak flow between 0.34 and ~6 m^3/s with variable duration between 1 and 26 days (Table 2, Fig. 2). Event A occurred on 23 October 2015, soon after leaf fall, and had a peak discharge (Q) of 0.34 m^3/s, which was equivalent to 0.1 of Q_{bf}. High flow event B occurred 2 weeks after event A and was roughly twice as large with a peak Q of 0.69 m^3/s ($0.2Q_{bf}$). Flow event C — the highest during our period of record — occurred between 3 December 2015 and 29 December 2015 (Table 2). Flow was elevated for the duration of this period with several individual peaks present over the 26-day period. The maximum peak Q was outside the range of the rating curve but was estimated to be ~6 m^3/s based on the rating curve and a flow resistant equation (Ferguson, 2007). Field observations and time-lapse photography coupled with measured stage indicate that the overbank conditions during this event lasted less than one day (~18 h). Five additional high flow events (D–I) occurred after event C during the winter period between 12 January 2016 and 21 March 2016. Peak Q and duration for these events ranged from 0.49 to 1.91 m^3/s and from 2 to 11 days respectively (Table 2). Discharge in February was lower than in December and January with only two moderate (0.49–0.56 m^3/s) high flow events (F and G). The last two high flow event (H and I) reached 1.46 and 1.06 m^3/s on 13 March 2016 and 21 March 2016 and lasted 4 and 2 days respectively (Table 2).

3.2. Shear stress variability

The magnitude and variability of shear stress (τ) during high flow events was investigated using a 2D hydraulic model (McDonald et al., 2006). The model was used to characterize flow field conditions during seven different flow levels from 0.4 to 3.4 m^3/s ($0.12Q_{bf}$-Q_{bf}). Mean shear stress increased with flow level from 18.3 N/m^2 when discharge was 0.40 m^3/s to 51.12 N/m^2 when discharge was 3.4 m^3/s (Table 3). Maximum τ ranged from 58.1 to 163 N/m^2. Shear stress was highly variable throughout the reach for each of the modeled flows (Fig. 3). The spatial distribution of τ values indicated a strong influence of bed topography with low τ (0–10 N/m^2) near the shallow bank boundaries for all of the modeled flows (Fig. 3). The highest τ values in all cases were found within and immediately downstream of the meander bend directly above the Chl-*a* sampling grid. This location corresponds with a pool formed against cohesive clay banks that constrain the flow into a small, deep, and stable portion of the stream. Shear stress values decrease along the straight portion of the stream but are highest in riffle areas. These seven modeled flow levels ($0.12Q_{bf}$-Q_{bf}) were used to characterize the flow field conditions during storms A-I (Fig. 2) and to quantify channel bed disturbance in all 18 instances in which Chl-*a* was measured (Table 3).

The spatial τ estimates were coupled with grain size fractions (D_2, D_{50}, and D_{84}) to calculate the likelihood of sediment scouring. The percentage of the channel bed experiencing shear stress values capable of mobilizing each size fraction (i.e., $\tau_i^*/\tau_r^* \geq 1$) increased with Q (Table 3). For the 0.4 m^3/s flow 31.4, 7.7, and 4.8% of the area had $\tau_i^*/\tau_r^* \geq 1$ for the D_2, D_{50}, and D_{84} respectively. For the highest modeled flow (3.4 m^3/s), these areas increased in size to 79, 70.4, and 66.4% (Table 3).

The spatial distribution of τ_i^*/τ_{ri}^* values was used to designate disturbance categories for nodes of the Chl-*a* grid. The disturbance

Table 2
High flow events (A–I) magnitude, duration, and size relative to bankfull (Q_{bf}) flow; the modeled flow use to characterize shear stress (τ) is also indicated

High flow event	Dates	Duration (days)	Peak discharge (Q) (m^3/s)	Fraction of Q_{bf}	Modeled Q used to characterize τ
A	30 October 2015–31 October 2015	2	0.34	0.1	0.40
B	16 November 2015–20 November 2015	4	0.69	0.2	0.64
C[a]	3 December 2015–29 December 2015	26	6.0[b]	1.7	3.4
D	12 January 2016–22 January 2016	10	1.91	0.6	1.91
E	29 January 2016–31 January 2016	2	1.29	0.4	1.3
F	14 February 2016–15 February 2016	1	0.49	0.15	0.40
G	19 February 2016–20 February 2016	1	0.56	0.16	0.64
H	13 March 2016–17 March 2016	4	1.46	0.43	1.5
I	21 March 2016–23 March 2016	2	1.06	0.31	0.99

[a] This consisted of a series of high flows between 1.3 and ~6 m^3/s.
[b] Estimated.

Please cite this article as: Katz, S.B., et al., The influence of channel bed disturbance on benthic Chlorophyll *a*: A high resolution perspective, Geomorphology (2017), https://doi.org/10.1016/j.geomorph.2017.11.010

Table 3
Modeled mean and maximum shear stress (τ) and percentage of channel bed with Shield stress above the reference for motion of the 2nd, 16th, and 84th percentiles of the grain size distribution for seven flows ($Q_i = 0.4$–3.4 m^3/s) considering the completed modeled domain and the Chl-*a* sampling grid

Q (m^3/s)	All modeled domain				Within sampling grid				
	τ mean (N/m^2)	τ max (N/m^2)	$\tau^*/\tau^*_{r2} \geq 1$ (% of bed)	$\tau^*/\tau^*_{r50} \geq 1$ (% of bed)	$\tau^*/\tau^*_{r84} \geq 1$ (% of bed)	τ range (N/m^2)	$\tau^*/\tau^*_{r2} \geq 1$ (% of bed)	$\tau^*/\tau^*_{r50} \geq 1$ (% of bed)	$\tau^*/\tau^*_{r84} \geq 1$ (% of bed)
0.40	18.34	58.12	31.4	7.7	4.8	2.43–56.39	40.6	15.6	8.8
0.64	23.10	75.80	50.2	20.3	12.1	2.07–69.25	58.0	34.1	25.0
0.99	24.62	83.29	54.2	24.5	16.7	2.02–74.06	62.5	40.9	32.4
1.33	25.60	81.72	57.0	28.3	19.8	2.96–75.25	67.0	45.2	36.4
1.46	26.16	80.87	58.2	30.2	21.2	2.47–76.89	69.9	47.4	39.2
1.91	32.76	106.65	68.6	48.4	38.5	4.83–104.69	82.1	64.5	55.1
3.40	51.12	163.06	79.0	70.4	66.4	19.38–158.69	99.4	95.7	92.9

classification within the Chl-*a* sampling grid varied between flows (Table 3, Fig. 3). For example, the high disturbance classification for the D_{50} corresponds to the yellow, orange, and red areas in Fig. 3. In general, we observed a region of high disturbance along the center of the sampling grid for all D_i, which grew in size with increasing Q and decrease D_i; from 8.8–40.6% of the Chl-*a* grid for the 0.4 m^3/s flow to 93.9–99.4% for the 3.4 m^3/s event (Table 3). Areas of low disturbance were found in general along the edges and within the lower portion of the Chl-*a* grid, which corresponds to the banks and the head of a small pool at the downstream end of the grid (Fig. 3). Putting these results in context with the hydrograph indicates that during flow events A and B (0.34 and 0.69 m^3/s respectively) high disturbance nodes in the Chl-*a* sampling grid occupied 40.6–58%, 15.6–34.1%, and 8.8–25% of the bed considering the D_2, D_{50}, D_{84} respectively and the modeled flows 0.4–0.64 m^3/s (Table 3). During the highest flow event (C, ~6 m^3/s) >93.9% of the Chl-*a* sampling grid experienced high disturbance according to all grain sizes considering the model results for a 3.4-m^3/s event (Table 3). For the remaining winter high flow events (D–G), the percentage of the bed exposed to high disturbance varied 25–82.1% considering all grain sizes and the model results from flows 0.64 to 1.91 m^3/s (Table 3); while for the early spring event (H) high disturbance characterized 69.9, 47.4, and 39.2% of the bed for the D_2, D_{50}, D_{84} respectively, considering the modeling results for a 1.46-m^3/s event (Table 3).

3.3. Chlorophyll-a and channel bed disturbance

We collected 1466 measurements of Chl-*a* (each with 5 replicates) over 18 sampling periods (Table 4). Overall, estimated grid cell Chl-*a* values ranged from 0.02 and 176 mg/m^2. Mean Chl-*a* concentration estimates among disturbance levels and sampling dates varied between 0.14 and 59 mg/m^2 (Table 4). We paired each sampling time with the modeled τ values for the immediately preceding high flow event (Fig. 2). We found that the mean shear stress in the channel bed explained 49% of the variance in measured Chl-*a* concentrations among data points on the streambed (Fig. 4A). The relation between mean τ during the previous storm event and mean Chl-*a* for the 18 sampling occasions together is strongly described by an exponential relation (Chl-*a* = $600e^{-0.11\tau}$, $r^2 = 0.86$, *p*-value < 0.001; Fig. 4B). Based on the 2D shear stress results we were able to investigate the effect that movement of different size fractions had on Chl-*a* (Fig. 5). We found similar relations for large (D_{84}), medium (D_{50}), and small particles (D_2), indicating that at Oak Creek abrasion and the saltation of large particles control biomass accrual. All the relations between the fraction of the bed with $\tau^*_i/\tau^*_{ri} > 1$ and Chl-*a* were exponential and strong ($r^2 = 0.71$–0.87, *p*-value < 0.0001, Fig. 5). However, the movement of the smallest grains (D_2) depicted a steeper (i.e., higher slope; Fig. 5C) relation according to which, once 92% of the bed experienced shear stress values above the reference for motion of the D_2, the Chl-*a* was consistently <0.6 mg/m^2. This threshold was lower for the D_{50} and D_{84} and indicated that Chl-*a* < than 0.6 mg/m^2 when the movement of these particles was likely to occur in 67 and 81% of the bed. In sum, disturbance driven by bedload movement greatly controls the amount of Chl-*a* that is removed (and conversely that persists). Indeed, considering the likelihood of the movement of each fraction, we found significant differences in Chl-*a* between disturbance levels in 12–14 of the 18 sampling dates that were collected before and after high flow events (Fig. 2, Table 4). No comparison was possible for the three sampling dates immediately after the highest peak flow (event C) because no sampling locations were classified as low disturbance for any of the size fractions. This flood resulted in shear stress values that were capable of mobilizing the D_2, D_{50}, and D_{84} in 99.4, 95.7, and 92.9% of the sampling grid respectively (Table 3) indicating that ecological resilience from refuge of undisturbed substrates is lost during the most extreme flow conditions. Across the 12–14 instances in which a significant difference in Chl-*a* between disturbance patches was detected 7, 8, and 8 had post-disturbance Chl-*a* values greater in the low disturbance grid cells relative to the high disturbance grid cell locations considering disturbance thresholds defined based on the D_2, D_{50}, and D_{84} respectively. Conversely, we found 5, 6, and 6 sampling events in which the mean Chl-*a* concentrations were greater in the high disturbance category considering disturbance thresholds defined based on the D_2, D_{50}, and D_{84} respectively (Table 4).

The temporal variation of Chl-*a* concentrations during the study period can be characterized by periods of biomass loss immediately following high flow events and periods of biomass accrual between high flow events (Fig. 6). The lowest measured mean concentrations occurred following the highest flow event of sampling period, which was also the highest event of the year (event C: between 4 January 2016 and 26 January 2016 with Chl-*a* concentrations <0.36 mg/m^2; Table 4).

In addition to variability in scour and the loss of benthic periphyton, variability in the recovery (resilience) of benthic periphyton also observed. The highest measured mean concentrations occurred in the high disturbance areas (defined based on the movement of any of the grain sizes considered) during relatively long recovery periods following relatively low flow events in 13 November1 2015, 13 days after a 0.1Q_{bf} event when Chl-*a* reached 50, 59, and 46.8 mg/m^2 and in 29 February 2016, 9 days after a 0.16Q_{bf} event when Chl-*a* reached 39.5, 37.7, and 48.3 mg/m^2 considering the likelihood of the movement of the D_2, D_{50}, and D_{84} respectively (Fig. 6A–C). This suggests an upper limit of Chl-*a* concentration. Indeed, areas of low disturbance also reached an upper boundary in Chl-*a* levels around ~35 mg/m^2 (Table 4, Fig. 6A–C).

Considering all size fractions (D_2, D_{50}, and D_{84}), the patterns of Chl-*a* concentrations in areas of high and low disturbance were similar (Fig. 6A–C). This pattern indicated that the susceptibility of Chl-*a* concentrations to disturbance by high flow events was dependent on the state of recovery of the algal community at the time of the disturbance and not solely the size distribution of mobilized sediment. For example, considering the D_{50}, Chl-*a* concentrations increased consistently in regions of high and low disturbance from 14 to 630% following high flow events when pre-disturbance Chl-*a* concentrations were <25.4 mg/m^2 (Table 4). These increases occurred primarily in the winter when high flow events were relatively frequent (Fig. 2). Specifically, Chl-*a* increased following high flow events E–G, 0.14–0.38Q_{bf} (sampling dates 8 February 2016, 15 February 2016, 22 February 2016, and 29 February 2016), as well as in 30 November 2015 after a 0.2Q_{bf} event. Mean

Please cite this article as: Katz, S.B., et al., The influence of channel bed disturbance on benthic Chlorophyll *a*: A high resolution perspective, Geomorphology (2017), https://doi.org/10.1016/j.geomorph.2017.11.010

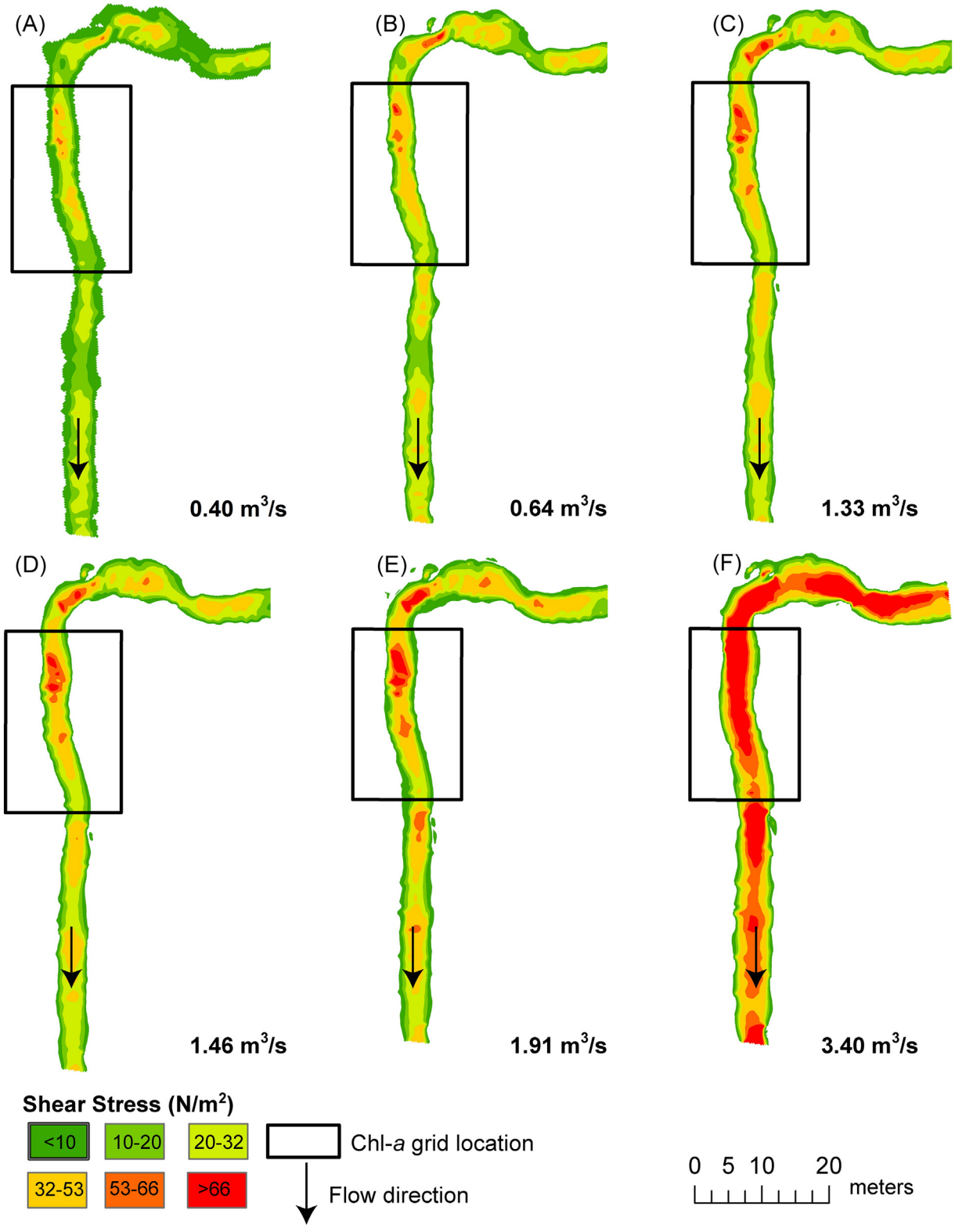

Fig. 3. Shear stress (τ) distributions for six of the modeled flows between 0.4 and 3.4 m^3/s ($0.1Q_{bf}$-Q_{bf}).

Chl-*a* concentrations across the bed consistently increase between 4 January 2016 and 29 February 2016 after the highest flow event ($1.7Q_{bf}$, event C) despite the occurrence of two high flow events ($0.6Q_{bf}$ and $0.4Q_{bf}$ respectively) on 12 January 2016 and 29 January 2016. In other words, these two high flows that ranked 2nd and 4th of the 9 in terms of flow magnitude did not create a noticeable decrease in Chl-*a* concentrations in either high or low disturbance regions. Chl-*a* decreased in high and low disturbance regions (defined based on the D_{50}) of the streambed in 20 November 2016, 4 January 2016, 19 March 2016, and 31 March 2016. The Chl-*a* concentrations prior to these dates were above the 40th percentile of the Chl-*a* distribution (15.91 mg/m^2). The percent decrease associated with storm events ranged from 8 to 99%, with the greatest depletions registered in 4 January 2016 following the largest flood ($1.7Q_{bf}$). The identified thresholds

Please cite this article as: Katz, S.B., et al., The influence of channel bed disturbance on benthic Chlorophyll *a*: A high resolution perspective, Geomorphology (2017), https://doi.org/10.1016/j.geomorph.2017.11.010

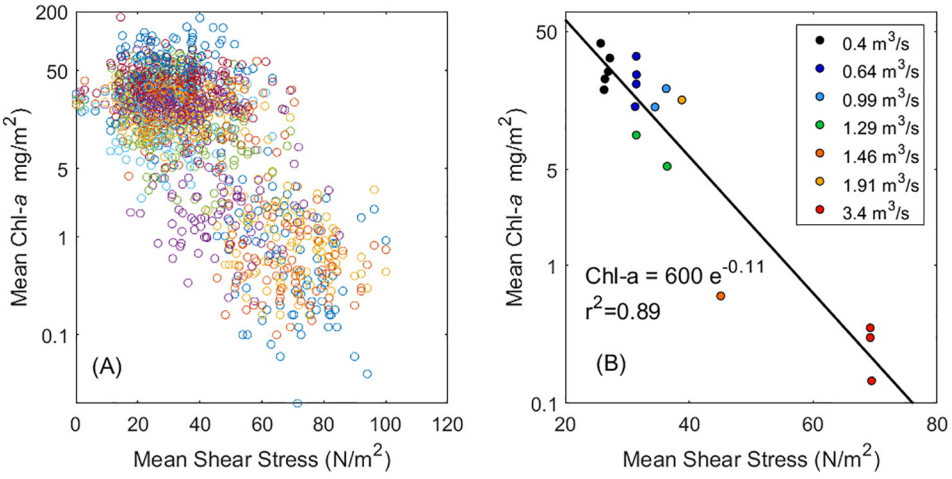

Fig. 4. Relationship between shear stress and Chl-*a* during 18 sampling events. (A) All measurements and (B) mean values of shear stress and Chl-*a* per sampling date.

indicated that Chl-*a* consistently increased after a high flow event when preceding Chl-*a* values are <~15 mg/m^2 and that Chl-*a* consistently decreases after a high flow event when preceding Chl-*a* > 29 mg/m^2. Thus, increases and decreases of Chl-*a* were observed when preceding Chl-*a* was 15–29 mg/m^2. This is also reflected in different accrual rates between the winter and fall periods.

Although the temporal patterns of Chl-*a* accrual and depletion are similar considering the relative movement of different grain sizes (Fig. 6A–C), we found contrasts in the magnitude of the difference in Chl-*a* between high and low disturbance. For example, in 26 January 2016, 8 February 2016, and 15 February 2016, Chl-*a* in the low disturbance areas was 1.5–2.9 higher than in the high disturbance (defined based on the D_2) compared to 1.2–2.1 times more Chl-*a* in the low disturbances vs. the high disturbance based the D_{84} (Fig. 6D). These instances occurred after high winter flows when abrasion by small particles (represented here by the D_2) likely played a significant role in the Chl-*a* disturbance regime. Conversely, the movement of coarse material played a more significant role in 23 October 2015, 6 November 2015, and 19 March 2016. In these dates, Chl-*a* in the low disturbance was 1.2–1.4 higher than in the high disturbance (defined based on D_{84}) compared to 0.64 and 1.2 times more Chl-*a* in the low disturbances vs. the high disturbance based on the D_2 (Fig. 6D).

The doubling time for the period preceding the 1.7Q_{bf} event between 23 October 2015 and 13 November 2015 was 15 and 31 days for the low and high disturbance areas (based on D_{50}) respectively. We found similar results based on disturbance categories defined with the D_2 (19 and 29 days) and the D_{84} (18 and 22 days). Finally, the doubling time was 3 times shorter in the winter time (5 days, considering mean Chl-*a* concentrations between 4 January 2016 and 11 January 2016, when preceding Chl-*a* was <1 mg/m^2) than in the fall (16 days, considering mean Chl-*a* concentrations across high and low disturbance areas between 2 November 2015 and 13 November 2015 when preceding Chl-*a* was 17 mg/m^2) demonstrating the inverse relation between channel bed disturbance intensity and Chl-*a* accrual rate.

3.4. Nutrients, temperature, and light

We considered the influence of other factors on the observed variability of Chl-*a*. Nutrient concentrations ranged from 4.8 to 102.4, 4 to 39, and 6.4 to 38.6 μg/L for nitrate, ammonia, and phosphate respectively. Nitrate concentrations were on average 45 μg/L and consistently below 63 μg/L except in November 2015 after flow event A when nitrate concentration was >100 μg/L. Temperature varied between 1.8 and 14.9°C, and light varied between 0.27 and 11.3 mol/m^2. These are factors that affect overall periphyton accrual, but in this stream they do not vary at the small spatial scales at which we were quantifying patterns of algal standing stocks. Nutrient concentrations and temperature were uniform within the Chl-*a* sampling grid considering the fact that the flow

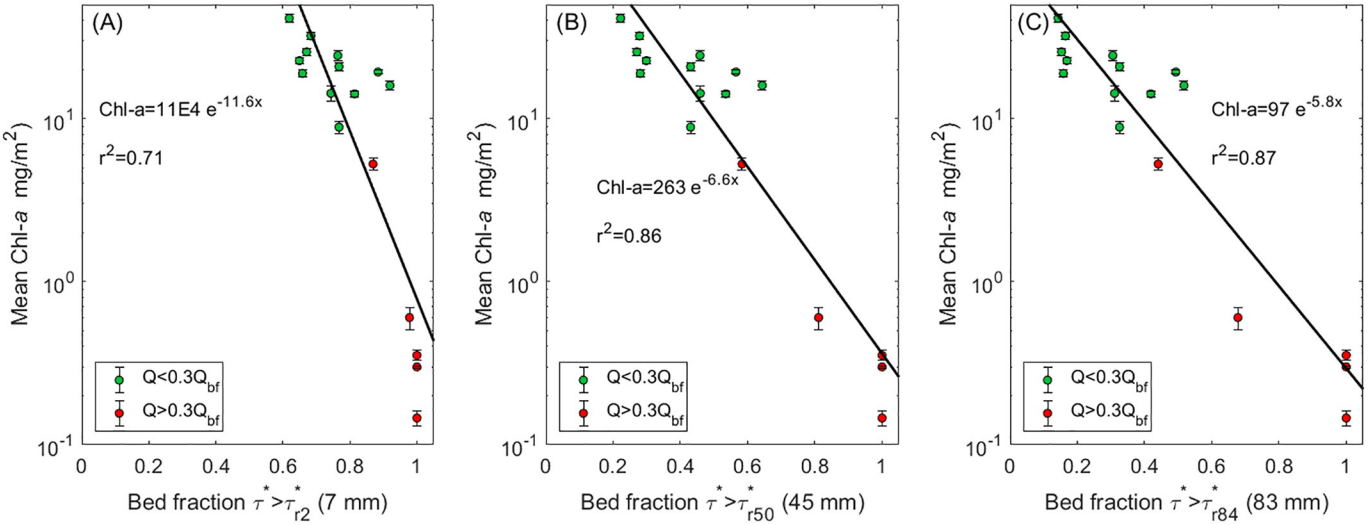

Fig. 5. Relationship between the percentage of bed with shear stress above the reference for movement of the D_2 (A), D_{50} (B), and D_{84} (C) and for mean Chl-*a* per sampling date.

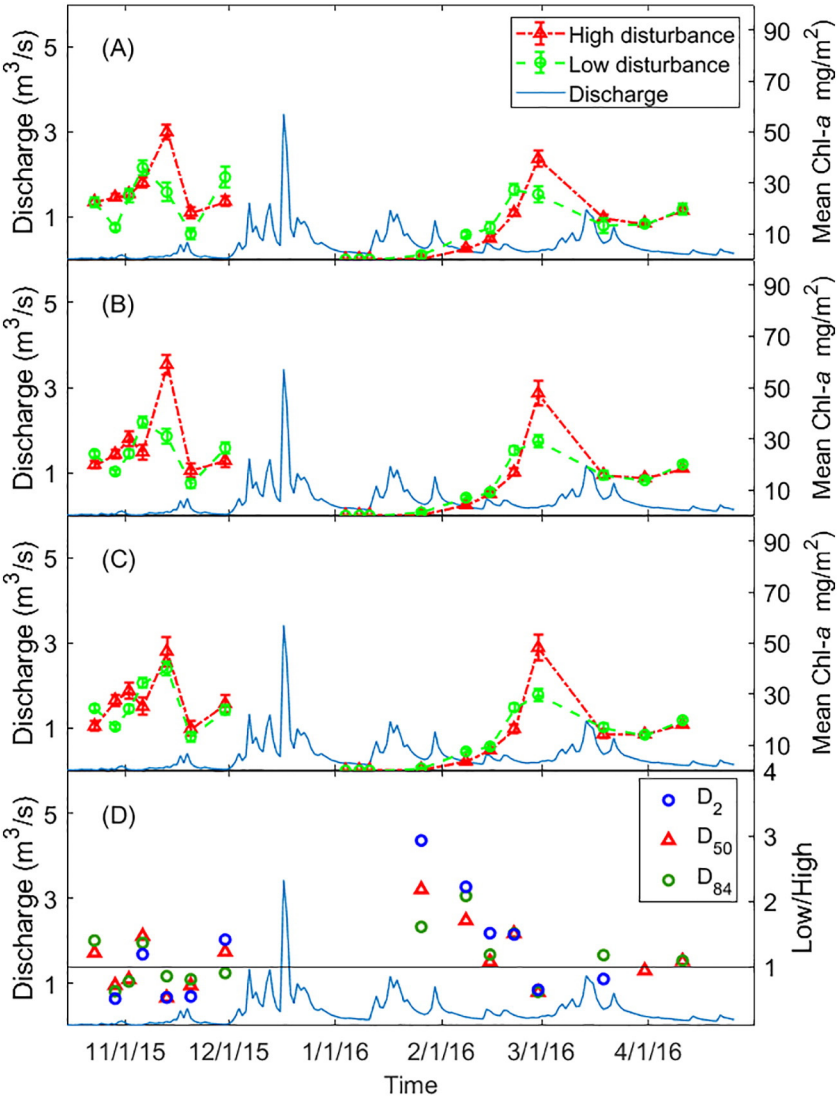

Fig. 6. Mean Chlorophyll-*a* (Chl-*a*) measurements for low and high areas of disturbance defined based on the threshold for motion of the D_2 (A), D_{50} (B), and D_{84} (C) in Oak Creek, OR, between 16 October 2015 and 11 April 2016. (D) Presents the ratio of Chl-*a* in the low to high disturbance areas for instances with significant differences between the two disturbance categories considering the movement of the D_2, D_{50}, and D_{84}.

was very well mixed. Light could potentially explain some of the observed spatial variability (Heaston et al., 2017; Warren et al., 2017). However, shading conditions within the sampling grid are relatively uniform in this system in winter when few leaves are on the tree and therefore fewer localize sunflecks develop. Overall, given the Mediterranean climate with wet winters, most days were cloudy throughout the winter sampling period. In an assessment of correlations between nutrients (nitrate, ammonia, and phosphate), PAR, and water temperature and mean Chl-*a*, all yielded weak nonsignificant relationships ($r^2 < 0.2$ and *p*-values > 0.3).

4. Discussion

The goal of this study was to investigate the relationship between the spatial variability of shear stress and the spatial variability of benthic Chl-*a* loss and recovery following moderate and large discharge events in a headwater stream. In addition to recovery rates, spatial variability in scour was expected to illustrate how the heterogeneous environment of streams can promote resilience to more moderate events by creating areas with low shear stress where benthic periphyton can persist. After coupling 2D estimates of shear stress values for a wide range of flows with measurements of benthic photosynthetic pigments (used as a surrogate for Chl-*a* and collected at the same high spatial resolution before and shortly after nine separate winter storm events), we found that spatial variability in localized shear stress that develops during more moderate storm events can yield spatially variable benthic algal abundances.

We observed an inverse relation between the relative movement of particles of different sizes (i.e., D_2, D_{50}, and D_{84}) and Chl-*a* for most sampling dates after relatively high discharge storm events (0.4–1.7 of bankfull discharge). This supported our expectation that areas of elevated shear stress would be disproportionally impacted by high flow events. However, in contrast to our expectations, the high shear stress locations were not universally lower in periphyton standing stocks, and spatial variability in flow appeared to influence the recovery of the system. During the recovery period (particularly long recovery periods) higher shear stress areas appeared to accumulate periphyton at a faster rate than the low shear stress areas thereby demonstrating greater recovery (engineering resilience) as well as greater initial susceptibility to higher flows. Further, the antecedent conditions and phase of recovery from prior events modulated the effects of the local shear stress and the relative effect of the movement of different grain sizes. These regions of high shear stress are particularly dynamic in regard to periphyton abundance not only in loss but also in recovery.

Please cite this article as: Katz, S.B., et al., The influence of channel bed disturbance on benthic Chlorophyll *a*: A high resolution perspective, Geomorphology (2017), https://doi.org/10.1016/j.geomorph.2017.11.010

Table 4
Summary of benthic Chlorophyll-*a* (Chl-*a*) measurements taken on 18 sampling dates between 23 October 2015 and 11 April 2016: the total number of grid cells sampled (*n*), mean and standard deviation (std) of the Chl-*a* concentrations (Chl-a_{mean}, Chl-a_{std}) are given for grid cells classified as low ($\tau_i^*/\tau_{ri}^* < 1$) and high ($\tau_i^*/\tau_{ri}^* \geq 1$) disturbance categories for the D_2, D_{50}, and D_{84}; the Student's *t*-test *p*-value comparing Chl-*a* between low and high disturbance during each sampling date are also presented.

Date	D_2									D_{50}			
	Low disturbance ($\tau^*/\tau_i^* < 1$)				High disturbance ($\tau^*/\tau_i^* \geq 1$)				*t*-Test	Low disturbance ($\tau^*/\tau_i^* < 1$)			
	n	Chl-*a* mean (mg/m^2)	Chl-*a* std. (mg/m^2)	% change	n	Chl-*a* mean (mg/m^2)	Chl-*a* std. (mg/m^2)	% change	*p*-Value	n	Chl-*a* mean (mg/m^2)	Chl-*a* std. (mg/m^2)	% change
23-Oct-15	27	22.54	2.00	0.00	50	22.69	1.12	0.00	0.6747	54	24.18	1.22	0.00
29-Oct-15	28	12.54	1.29	−0.44	54	24.45	1.20	0.08	<0.0001	59	17.25	1.01	−0.29
2-Nov-15	28	25.27	2.61	1.02	57	25.76	1.56	0.05	0.2815	62	24.23	1.53	0.40
6-Nov-15	25	36.04	2.97	0.43	54	30.21	2.09	0.17	<0.0001	57	36.44	2.15	0.50
13-Nov-15	24	26.52	3.75	−0.26	39	50.03	2.92	0.66	<0.0001	49	30.99	2.89	−0.15
20-Nov-15	19	10.13	2.10	−0.62	55	18.56	2.14	−0.63	<0.0001	40	12.58	1.84	−0.59
30-Nov-15	17	32.34	4.20	2.19	55	22.84	1.83	0.23	<0.0001	39	26.45	2.22	1.10
4-Jan-16	–	0.00	0.00	–	86	0.15	0.02	−0.99	–	–	0.00	0.00	–
8-Jan-16	–	0.00	0.00	–	87	0.30	0.00	1.06	–	–	0.00	0.00	–
11-Jan-16	–	0.00	0.00	–	87	0.35	0.03	0.18	–	–	0.00	0.00	–
26-Jan-16	2	1.75	1.44	0.00	88	0.60	0.09	0.69	<0.0001	17	1.24	0.41	0.00
8-Feb-16	11	9.80	1.16	4.60	73	4.41	0.50	6.39	<0.0001	35	7.08	0.75	4.72
15-Feb-16	20	12.59	2.12	0.28	66	8.31	0.82	0.88	<0.0001	49	9.21	1.11	0.30
22-Feb-16	20	27.46	2.05	1.18	66	18.37	1.25	1.21	<0.0001	49	25.55	1.59	1.77
29-Feb-16	20	25.63	3.20	−0.07	66	39.55	2.97	1.15	<0.0001	49	29.18	2.45	0.14
19-Mar-16	7	13.29	3.10	−0.48	80	16.35	1.18	−0.59	<0.0001	31	15.91	1.72	−0.45
31-Mar-16	16	14.02	1.08	0.05	70	14.25	0.70	−0.13	0.2831	40	13.84	0.76	−0.13
11-Apr-16	8	19.77	2.08	0.41	61	19.25	0.60	0.35	0.1167	30	20.07	0.81	0.45

Over longer periods, rapid loss and recovery of Chl-*a* in high shear stress areas combined with reduced loss and also reduced recovery rates in the low shear stress areas are likely to interact to create more consistent reach-scale Chl-*a* abundances during the winter in this system when moderate discharge events occur regularly. However, the largest event in our study period demonstrated that fluvial disturbances mobilizing most of the streambed particles can override this potential mechanism for ecological resilience and can significantly reduce benthic algal Chl-*a* concentrations throughout an entire reach. In this case, the faster recovery rates in the high shear stress regions were the key factors in providing resilience to the system.

The applicability of 2D modelling to small mountain streams has grown in recent years (e.g., Cienciala and Hassan, 2013; Segura and Pitlick, 2015; Monsalve et al., 2016) increasing the potential to better understand complex sediment transport and channel evolution processes and to investigate the influence of channel bed disturbance in headwater stream ecosystems (Segura et al., 2011). Traditionally, bed disturbance has been characterized based on metrics of discharge (Fisher et al., 1982; Biggs and Close, 1989; Townsend and Douglas, 2014), one-dimensional (1D) estimates of substrate mobility (Uehlinger et al., 1996; Biggs et al., 1999; Hoyle et al., 2017), or spatial patterns of scour and fill (Matthaei et al., 2003; Luce et al., 2013). Because these metrics do not account explicitly for the spatial variability of shear stress and oversimplify sediment transport processes within a reach, they are not able to identify the underlying disturbance processes. Our flow modeling results indicate heterogeneous flow field conditions in Oak Creek across all modeled flows ($0.1Q_{bf}$-Q_{bf}). The range of modeled shear stress values had the potential to mobilize the D_2, D_{50}, and D_{84} in 31.4–79, 7.7–70, and 4.8–70.4% of the channel bed respectively. In the absence of this 2D perspective and based solely on mean shear stress values (1D approach), we would have found a binary disturbance response variable (0% or 100%), which would have yielded only two unstable events (both $>0.56Q_{bf}$) able to mobilize the D_{50} and D_{84}, while all events would have been able to mobilize the D_2. Indeed, a 1D approach would have missed the large shear stress variability we reported where areas of the bed exhibited values up to almost 6 times the reference value for motion for the D_{50}, even though the mean value was not even 2 times, as well as the exponential relations we found for the individual size fractions (Fig. 5). Our study is a step forward from previous attempts not only because we considered a 2D approach to describe the flow field (Segura et al., 2011) but also because we were able to conduct high resolution in situ measurements of benthic Chl-*a*. This is to our knowledge the first attempt to measure the flow field and benthic algae at high resolution at the reach scale.

Our results indicated that channel bed disturbance considering the movement of the D_2, D_{50}, and D_{84} explains a large proportion of the benthic Chl-*a* variability. Although this relation was negative overall (i.e., lower Chl-*a* values associated to high disturbance), in some instances Chl-*a* was significantly higher in channel bed locations associated with high disturbance (defined based on any grain size) than in nearby low disturbance sites. While the mechanism by which high disturbance could be associated to low Chl-*a* is relatively clear: high velocity and shear stress removing biofilm cells from the rock surfaces (Biggs and Close, 1989; Biggs et al., 1999), the mechanisms by which high Chl-*a* is associated to high disturbance is less straightforward. In our study, this was the case on 29 October 2015, 2 November 2015, 13 November 2015, 20 November 2015, 29 February 2016, and 31 March 2016 independent of the grain size used to define disturbance. Most of these were sampling dates in the fall prior to the largest flow event ($1.7Q_{bf}$) or during relatively calm periods in the winter where algal communities were allowed to recover unabated by large flow events. During these events, we hypothesize that the removal of large senescence biofilm communities and higher mass transfer in the higher velocity microhabitats led to the improvement of habitat conditions for rapid algal cell colonization and growth. Thus, the disturbance history appears to play an important role in the benthic Chl-*a* dynamics in this temperate-rainfall system. Although the temporal trends of Chl-*a* accrual in low and high disturbance patches were similar considering the movement of different sediment sizes, we found evidence that after the large storm events in the winter (26 January 2016 to 15 February 2016) abrasion was significantly more relevant for Chl-*a* accrual than the saltation of coarse particles. During this period, the areas of low disturbances (i.e., no movement of D_2) had 1.5–2.9 more Chl-*a* compared to 1.1–2.1 for the low disturbed areas considering coarse material (D_{50} and D_{84}). One possible explanation for this more drastic contrast between low and high disturbance patches could be a reflection of the greater availability of fine sediment within the channel bed following a large flow event (i.e., event C) than after more moderate events. Indeed, input of fresh fine sediment from bank erosion or mobilization of the armor layer in the bed is possible during large events.

Our data supports the importance of understanding algal abundances prior to a disturbance event when determining the response of

Please cite this article as: Katz, S.B., et al., The influence of channel bed disturbance on benthic Chlorophyll *a*: A high resolution perspective, Geomorphology (2017), https://doi.org/10.1016/j.geomorph.2017.11.010

D_{84}														Overall mean
High disturbance ($\tau^*/\tau_i^* \geq 1$)				*t*-Test	Low disturbance ($\tau^*/\tau_i^* < 1$)				High disturbance ($\tau^*/\tau_i^* \geq 1$)				*t*-Test	
n	Chl-*a* mean (mg/m^2)	Chl-*a* std. (mg/m^2)	% change	*p*-Value	*n*	Chl-*a* mean (mg/m^2)	Chl-*a* std. (mg/m^2)	% change	*n*	Chl-*a* mean (mg/m^2)	Chl-*a* std. (mg/m^2)	% change	*p*-Value	Chl-*a* mean (mg/m^2)
23	19.95	1.62	0.00	<0.0001	64	24.52	1.14	0.00	13	17.49	1.89	0.00	<0.0001	22.65
23	24.06	1.78	0.21	<0.0001	69	17.28	0.96	−0.30	13	27.69	2.21	0.58	<0.0001	18.92
23	30.06	2.72	0.25	<0.0001	72	24.30	1.48	0.41	13	31.32	3.07	0.13	<0.0001	25.63
22	24.81	2.81	−0.17	<0.0001	66	34.41	1.97	0.42	13	25.19	3.44	−0.20	<0.0001	32.14
14	58.96	3.82	1.38	<0.0001	54	40.10	2.51	0.17	9	46.83	5.81	0.86	<0.0001	41.15
34	17.65	2.59	−0.70	<0.0001	51	13.36	1.77	−0.67	23	16.55	2.80	−0.65	<0.0001	14.27
33	21.54	2.57	0.22	<0.0001	50	23.75	1.93	0.78	22	26.27	3.44	0.59	<0.0001	24.35
86	0.15	0.02	−0.99	–	–	0.00	0.00	–	86	0.15	0.02	−0.99	–	0.15
87	0.30	0.00	1.06	–	–	0.00	0.00	–	87	0.30	0.00	1.06	–	0.30
87	0.35	0.03	0.18	–	–	0.00	0.00	–	87	0.35	0.03	0.18	–	0.35
73	0.57	0.10	0.61	<0.0001	29	0.89	0.25	0.00	61	0.55	0.10	0.57	<0.0001	0.60
49	4.14	0.59	6.30	<0.0001	47	7.55	0.72	7.48	37	3.63	0.61	5.55	<0.0001	5.27
37	8.55	1.05	1.06	0.01	58	9.53	1.02	0.26	28	8.04	1.14	1.22	<0.0001	8.86
37	16.95	1.44	0.98	<0.0001	58	24.83	1.48	1.61	28	16.48	1.54	1.05	<0.0001	20.82
37	47.77	4.74	1.82	<0.0001	58	29.86	2.40	0.20	28	48.32	5.21	1.93	<0.0001	33.10
56	15.99	1.44	−0.67	0.81	42	17.07	1.46	−0.43	45	14.47	1.69	−0.70	<0.0001	15.96
46	14.70	0.93	−0.08	<0.0001	50	14.13	0.70	−0.17	36	14.31	1.08	−0.01	0.3577	14.18
39	18.48	0.83	0.26	<0.0001	35	19.85	0.71	0.41	34	18.16	1.01	0.27		19.29

the algal community to it — rather than using just post-disturbance data alone. For instance, events B and H had moderate peak discharge levels ($0.2Q_{bf}$ and $0.43Q_{bf}$ respectively), and after those events we measured a reduction in Chl-*a* concentrations. However, Chl-*a* concentrations increased following high flow events D, E, F, and G, which had comparable discharge (ranging from $0.16Q_{bf}$ to $0.56Q_{bf}$). Although flows were comparable between these two sets of events, mean Chl-*a* concentrations *prior* to the second set of events (D–G) was substantially lower (overall mean 0.35–8.86 mg/m^2) than for the first (B and H; 41.2–33.1 mg/m^2). High flow events D-G occurred following a complete reset of the channel bed and of the benthic algal community after a $1.7Q_{bf}$ flow, while events B and H occurred after periods of prolonged growth with relatively little disturbance. After event D in 26 January 2016, disturbance by saltation of coarse particles (D_{84}) only resulted in differences between low and high disturbance patches of 1.6 times, while for the D_2 the low disturbance areas had almost 3 times as much Chl-*a* as the high disturbances areas. Presumably, the community composition in the channel bed in which the shear stress is large enough to move large grains are more resistant to losses, whereas the channel bed areas in which the movement of D_2 is possible are more prone to biomass losses. Indeed, the results of other studies focusing on the resistance and succession of individual taxa that comprise algal communities can help explain the observed differences between these high flow events. Previous studies indicated that high resistance species are often more abundant in river patches subject to high velocity than in patches subject to low velocity (Peterson and Stevenson, 1992) and that different species have different levels of resilience (Schneck and Melo, 2012; Hart et al., 2013). In essence, early successional species such as diatoms show greater resistance to flood disturbance than late successional species such as filamentous algae because of differences in their growth forms (i.e., compact single cell diatoms vs. lengthy multicellular filamentous algae) (Stevenson, 1990; Peterson and Stevenson, 1992; Biggs and Thomsen, 1995; Davie and Mitrovic, 2014). Although we did not monitor species composition in the current study, our results are consistent with differences in growth form and susceptibility to subsequent scour; and the fundamental pattern of initial biomass muting storm responses holds for this mechanism as well.

The results of our study also show that the recovery of algal communities in the period following high flow events is dependent on the intensity and spatial extent of the disturbing event. For example, during the initial recovery period after a moderate flow ($0.1Q_{bf}$, event A), patches in the bed that did not experience mobilization of the D_2, D_{50}, or D_{84} (i.e., low disturbance) had faster Chl-*a* recovery rates (Fig. 6) than areas in which these size fractions were likely mobile (i.e., high disturbance). With faster recovery when storms were less frequent, these high shear stress locations could ultimately support higher Chl-*a* concentrations. By the end of the longer fall recovery period in our study system, biomass in high disturbance areas grew at a much faster rate with doubling times 1.2–2 times those in low disturbance areas (15–19 vs. 22–31 days). Overall doubling times were 2.3 longer during the fall vs. the winter. Possible mechanisms for these differences in recovery rates include increased nutrient flux and light availability (because of removal of dead biomass) in areas of elevated velocity. This interpretation is consistent with several studies (Stevenson, 1990; Peterson et al., 1994; Matthaei et al., 2003; Murdock et al., 2004; Townsend and Douglas, 2014) yet in contrast to many others (Biggs and Close, 1989; Uehlinger et al., 1996; Biggs et al., 1999; Bergey and Resh, 2006; Segura et al., 2011), which showed inverse relationships between resilience and disturbance. In our system, algal biomass in the areas more resistant to scour (lower shear stress) were less resilient in regard to recovery rates, whereas the areas more likely to scour (less resistance) had greater algal biomass resilience with a greater capacity to recover from disturbance. Frequent sampling during time periods between disturbance events was important in identifying this relationship along with adequate rates of recovery in the time periods without disturbance. Assuming Chl-*a* as a metric for ecosystem functions we found no evidence for a functional change in the benthic algal standing stocks response to the observed overbank flow event, highlighting the ecological resilience of this ecosystem. Given the dynamic nature of streams, the capacity for recovery from a high flow event is expected and has been observed in other studies. In a study with continuous measurements of stream gross primary production (GPP) throughout a full year, Roberts et al. (2007) found that GPP declined sharply in spring following a large storm event and that it took 5 days for GPP rates to return to pre-storm levels. Working in artificial stream channels, Gerull et al. (2012) found that recovery to pre-disturbance GPP took about 7 days; but others have demonstrated that it can take up to 2 weeks for GPP to recover to pre-storm levels (Dodds et al., 1996). And, Segura et al. (2011) reported lower Chl-*a* values in high disturbance areas between snowmelt in June up to mid-September in a high elevation system in Colorado; but in that system, even though recovery rates were similar to those we calculated here (12–26 days), biomass accrual never peaked

Please cite this article as: Katz, S.B., et al., The influence of channel bed disturbance on benthic Chlorophyll *a*: A high resolution perspective, Geomorphology (2017), https://doi.org/10.1016/j.geomorph.2017.11.010

or plateaued. This result also indicates that resilience of systems to scour in regard to recovery rates also depend on other factors such as stream temperature, light, and nutrient availability (Rosenfeld and Roff, 1991; Biggs et al., 1999; Houser et al., 2005; Uehlinger, 2006; Roberts et al., 2007).

The engineering resilience of an algal community (capacity to recover from disturbance) is dependent not only on the disturbance history or the inverse relation between resilience and disturbance frequency but also on the availability of abiotic resources such as light, temperature, and nutrients, as well as biotic interactions such as grazing pressure and community composition (Larned, 2010; Townsend and Douglas, 2014). We believe that frequent in situ sampling in a system with moderated (above freezing) winter temperatures and periodic disturbances provided an ideal system to explore the spatial variability in resistance to flood scour and resilience after the disturbance event. Typically, studies investigating the influence of disturbance on the resilience of benthic algae compare streams with different disturbance histories (Biggs et al., 1999), through flume experiments (Peterson and Stevenson, 1992; Peterson et al., 1994; Biggs et al., 1998; Coundoul et al., 2015) or most commonly by studying temporal changes in one stream with multiple disturbance events (Fisher et al., 1982; Power and Stewart, 1987; Biggs and Close, 1989; Stevenson, 1990; Uehlinger et al., 1996; Murdock et al., 2004; Davie et al., 2012; Snell et al., 2014; Townsend and Douglas, 2014). Differences in abiotic growth resources either among sites or within the same site at different times of the year may affect the growth rates of benthic algae, which complicates isolating the influence of disturbance processes. Our study design, however, allowed us to isolate the influence of bed disturbance on resilience of algal communities (algal abundance) with multiple post-treatment sampling events occurring in a nondestructive way. While we made every effort to control for the availability of these abiotic resources, variability in the species composition of grazer macroinvertebrates was possible. Future efforts could continue to include assessing the movement of different size fractions by coupling a modelling approach such as the one we conducted here with bedload measurements. Adding assessments of whole stream metabolism along with standing stocks of benthic periphyton would also be useful in quantifying the overall resilience (persistence during a disturbance and recovery) of gross primary production at the reach scale. An additional aspect that deserves attention in extrapolating these results to other systems is understanding the relative importance of sediment supply and underlying lithology in modulating the effect of the movement of different size fractions on primary production.

5. Conclusions

The resilience of benthic algal communities to disturbance from high flow events is significantly influenced by antecedent conditions and variability in the spatial and temporal patterns of streambed shear stress and sediment mobility. In this study, we coupled 2D hydraulic modeling with high resolution measurements of benthic Chlorophyll *a* (Chl-*a*) to investigate temporal and spatial variations in biomass in response to disturbance of benthic algae in a forested mountain stream. We found significant differences in mean Chl-*a* concentrations between disturbance levels in 14 of 18 sampling occasions. In contrast to our expectation, channel bed areas with high disturbance did not always have the lowest Chl-*a* concentrations. Instead, prior disturbance history and the state of Chl-*a* recovery influenced the response of Chl-*a* to channel bed disturbance. Algal biomass in areas with lower shear stress were generally more resistant to scour but generally were also less resilient (slower to recover), whereas the areas more likely to scour (with less resistance) generally had greater algal biomass resilience with a greater capacity to recover from disturbance. Ultimately, timing along with the inverse relationship between resiliency and disturbance frequency highlights the complexity of the process of benthic algal loss and recovery associated with high flow events. High resolution measurements of disturbance and frequent sampling during time periods between disturbance events was important in identifying this relationship along with adequate rates of recovery in the time periods without disturbance. This is a novel use of high resolution benthic algal sampling paired with a high resolution 2D hydraulic model and provides a step forward in the development of a framework to organize and predict the effects of disturbance in primary production in streams.

Acknowledgements

This work was funded in part by the National Science Foundation grant award # 1619700 and the USDA National Institute of Food and Agriculture; McIntire Stennis project OREZ-FERM-876. The authors would like to thank Dr. Gordon Grant for insightful discussions, the McDonald Dunn Forest Director, Dr. Stephen Fitzgerald, for logistical support in McDonald Dunn Forest, and Dr. Jim Kiser for topographic surveying assistance. Richard McDonald of the USGS provided very useful suggestions in the hydrodynamic model FasTMECH. Joey Tinker, Olivia Cantwell, Matt Kaylor, Brian VerWey, and Catalina Seufert helped immensely with field and lab work. Finally, we would like to thank the Editor, Richard A. Marston, Managing Guest Editor, David R. Butler, and an anonymous reviewer for providing very helpful, detailed comments on an earlier version of this manuscript.

References

Atkinson, B.L., Grace, M.R., Hart, B.T., Vanderkruk, K.E.N., 2008. Sediment instability affects the rate and location of primary production and respiration in a sand-bed stream. J. N. Am. Benthol. Soc. 27 (3), 581–592.

Bergey, E.A., Resh, V.H., 2006. Differential response of algae on small streambed substrates to floods. Am. Midl. Nat. 155 (2), 270–277.

Bernot, M.J., Sobota, D.J., Hall, R.O., Mulholland, P.J., Dodds, W.K., Webster, J.R., Tank, J.L., Ashkenas, L.R., Cooper, L.W., Dahm, C.N., Gregory, S.V., Grimm, N.B., Hamilton, S.K., Johnson, S.L., McDowell, W.H., Meyer, J.L., Peterson, B., Poole, G.C., Valett, H.M., Arango, C., Beaulieu, J.J., Burgin, A.J., Crenshaw, C., Helton, A.M., Johnson, L., Merriam, J., Niederlehner, B.R., O'Brien, J.M., Potter, J.D., Sheibley, R.W., Thomas, S.M., Wilson, K.Y.M., 2010. Inter-regional comparison of land-use effects on stream metabolism. Freshw. Biol. 55 (9), 1874–1890.

Biggs, B.J.F., Close, M.E., 1989. Periphyton biomass dynamics in gravel bed rivers - the relative effects of flows and nutrients. Freshw. Biol. 22 (2), 209–231.

Biggs, B.J.F., Stokseth, S., 1996. Hydraulic habitat suitability for periphyton in rivers. Regul. Rivers: Res. Manage. 12 (2–3), 251–261.

Biggs, B.J.F., Thomsen, H.A., 1995. Disturbance of stream periphyton by perturbations in shear-stress - time to structural failure and differences in community resistance. J. Phycol. 31, 233–241.

Biggs, B.J.F., Goring, D.G., Nikora, V.I., 1998. Subsidy and stress responses of stream periphyton to gradients in water velocity as a function of community growth form. J. Phycol. 34 (4), 598–607.

Biggs, B.J.F., Smith, R.A., Duncan, M.J., 1999. Velocity and sediment disturbance of periphyton in headwater streams: biomass and metabolism. J. N. Am. Benthol. Soc. 18, 222–241.

Bone, C., Moseley, C., Vinyeta, K., Bixler, R.P., 2016. Employing resilience in the United States Forest Service. Land Use Policy 52, 430–438.

Cardinale, B.J., Palmer, M.A., Swan, C.M., Brooks, S., Poff, N.L., 2002. The influence of substrate heterogeneity on biofilm metabolism in a stream ecosystem. Ecology 83 (2), 412–422.

Cattaneo, A., Kerimian, T., Roberge, M., Marty, J., 1997. Periphyton distribution and abundance on substrata of different size along a gradient of stream trophy. Hydrobiologia 354, 101–110.

Cienciala, P., Hassan, M.A., 2013. Linking spatial patterns of bed surface texture, bed mobility, and channel hydraulics in a mountain stream to potential spawning substrate for small resident trout. Geomorphology 197, 96–107.

Coundoul, F., Bonometti, T., Graba, M., Sauvage, S., Sanchez Pérez, J.M., Moulin, F.Y., 2015. Role of local flow conditions in river biofilm colonization and early growth. River Res. Appl. 31 (3), 350–367.

Davie, A.W., Mitrovic, S.M., 2014. Benthic algal biomass and assemblage changes following environmental flow releases and unregulated tributary flows downstream of a major storage. Mar. Freshw. Res. 65 (12), 1059–1071.

Davie, A.W., Mitrovic, S.M., Lim, R.P., 2012. Succession and accrual of benthic algae on cobbles of an upland river following scouring. Inland Waters 2 (2), 89–100.

Dodds, W.K., Hutson, R.E., Eichem, A.C., Evans, M.A., Gudder, D.A., Fritz, K.M., Gray, L., 1996. The relationship of floods, drying, how and light to primary production and producer biomass in a prairie stream. Hydrobiologia 333 (3), 151–159.

Ferguson, R., 2007. Flow resistance equations for gravel- and boulder-bed streams. Water Resour. Res. 43 (5), 12.

Fisher, S.G., Gray, L.J., Grimm, N.B., Busch, D.E., 1982. Temporal succession in a desert stream ecosystem following flash flooding. Ecol. Monogr. 52 (1), 93–110.

Francoeur, S.N., Biggs, B.J.F., 2006. Short-term effects of elevated velocity and sediment abrasion on benthic algal communities. Hydrobiologia 561, 59–69.

Please cite this article as: Katz, S.B., et al., The influence of channel bed disturbance on benthic Chlorophyll *a*: A high resolution perspective, Geomorphology (2017), https://doi.org/10.1016/j.geomorph.2017.11.010

Gerull, L., Frossard, A., Gessner, M.O., Mutz, M., 2012. Effects of shallow and deep sediment disturbance on whole-stream metabolism in experimental sand-bed flumes. Hydrobiologia 683 (1), 297–310.
Gregory, S.V., 1980. Effects of Light, Nutrients and Grazing on Periphyton Communities in Streams. Ph.D. Oregon State University, Corvallis 151 pp.
Hart, D.D., Biggs, B.J.F., Nikora, V.I., Flinders, C.A., 2013. Flow effects on periphyton patches and their ecological consequences in a New Zealand river. Freshw. Biol. 58 (8), 1588–1602.
Heaston, E.D., Kaylor, M.J., Warren, D.R., 2017. Characterizing short-term light dynamics in forested headwater streams. Freshwater Sci. 36 (2), 259–271.
Hodgson, D., McDonald, J.L., Hosken, D.J., 2015. What do you mean, 'resilient'? Trends Ecol. Evol. 30 (9), 503–506.
Hoellein, T.J., Tank, J.L., Rosi-Marshall, E.J., Entrekin, S.A., Lamberti, G.A., 2007. Controls on spatial and temporal variation of nutrient uptake in three Michigan headwater streams. Limnol. Oceanogr. 52 (5), 1964–1977.
Holling, C.S., 1973. Resilience and stability of ecological systems. Annu. Rev. Ecol. Syst. 4 (1), 1–23.
Holtgrieve, G.W., Schindler, D.E., Gowell, C.P., Ruff, C.P., Lisi, P.J., 2010. Stream geomorphology regulates the effects on periphyton of ecosystem engineering and nutrient enrichment by Pacific salmon. Freshw. Biol. 55 (12), 2598–2611.
Houser, J.N., Mulholland, P.J., Maloney, K.O., 2005. Catchment disturbance and stream metabolism: patterns in ecosystem respiration and gross primary production along a gradient of upland soil and vegetation disturbance. J. N. Am. Benthol. Soc. 24 (3), 538–552.
Hoyle, J.T., Kilroy, C., Hicks, D.M., Brown, L., 2017. The influence of sediment mobility and channel geomorphology on periphyton abundance. Freshw. Biol. 62 (2), 258–273.
Jowett, I.G., Biggs, B.J.F., 1997. Flood and velocity effects on periphyton and silt accumulation in two New Zealand rivers. N. Z. J. Mar. Freshw. Res. 31 (3), 287–300.
Kahlert, M., McKie, B.G., 2014. Comparing new and conventional methods to estimate benthic algal biomass and composition in freshwaters. Environ. Sci.: Processes Impacts 16 (11), 2627–2634.
Kanavillil, N., Balika, D., Kurissery, S., 2015. Edge effect: a catalyst of spatial heterogeneity in natural biofilms. Hydrobiologia 744 (1), 77–90.
Katz, S., 2016. Sediment Transport Modeling and Implications for Benthic Primary Producers in Oak Creek. OR. MS. Oregon State University, Corvallis, OR 180 pp.
Lake, P.S., Bond, N., Reich, P., 2007. Linking ecological theory with stream restoration. Freshw. Biol. 52 (4), 597–615.
Larned, S.T., 2010. A prospectus for periphyton: recent and future ecological research. J. N. Am. Benthol. Soc. 29 (1), 182–206.
Legleiter, C.J., Kyriakidis, P.C., McDonald, R.R., Nelson, J.M., 2011. Effects of uncertain topographic input data on two-dimensional flow modeling in a gravel-bed river. Water Resour. Res. 47, W03518.
Lisle, T.E., Nelson, J.M., Pitlick, J., Madej, M.A., Barkett, B.L., 2000. Variability of bed mobility in natural, gravel-bed channels and adjustments to sediment load at local and reach scales. Water Resour. Res. 36 (12), 3743–3755.
Luce, J.J., Cattaneo, A., Lapointe, M.F., 2010. Spatial patterns in periphyton biomass after low-magnitude flow spates: geomorphic factors affecting patchiness across gravel-cobble riffles. J. N. Am. Benthol. Soc. 29 (2), 614–626.
Luce, J.J., Lapointe, M.F., Roy, A.G., Ketterling, D.B., 2013. The effects of sand abrasion of a predominantly stable stream bed on periphyton biomass losses. Ecohydrology 6 (4), 689–699.
Matthaei, C.D., Guggelberger, C., Huber, H., 2003. Local disturbance history affects patchiness of benthic river algae. Freshw. Biol. 48, 1514–1526.
May, C.L., Pryor, B., Lisle, T.E., Lang, M., 2009. Coupling hydrodynamic modeling and empirical measures of bed mobility to predict the risk of scour and fill of salmon redds in a large regulated river. Water Resour. Res. 45, W05402.
McDonald, R.R., Nelson, J.M., Kinzel, P.J., Conaway, J.S., 2006. Modeling surface-water flow and sediment mobility with the multi-dimensional surface water modeling system (MD_SWMS). U.S. Geological Survey Scientific Investigations Report 6 pp.
McDonald, R.R., Nelson, J., Paragamian, V., Barton, G., 2010. Modeling the effect of flow and sediment transport on White Sturgeon spawning habitat in the Kootenai River, Idaho. J. Hydraul. Eng. ASCE 136 (12), 1077–1092.
Merwade, V.M., 2009. Effect of spatial trends on interpolation of river bathymetry. J. Hydrol. 371 (1–4), 169–181.
Merwade, V.M., Cook, A., Coonrod, J., 2008. GIS techniques for creating river terrain models for hydrodynamic modeling and flood inundation mapping. Environ. Model Softw. 23 (10−11), 1300–1311.
Milhous, R., 1973. Sediment Transport in a Gravel Bottomed Stream. PhD. Oregon State University 232 pp.
Monsalve, A., Yager, E.M., Turowski, J.M., Rickenmann, D., 2016. A probabilistic formulation of bed load transport to include spatial variability of flow and surface grain size distributions. Water Resour. Res. 52 (5), 3579–3598.
Murdock, J., Roelke, D., Gelwick, F., 2004. Interactions between flow, periphyton, and nutrients in a heavily impacted urban stream: implications for stream restoration effectiveness. Ecol. Eng. 22 (3), 197–207.
Nelson, J.M., Smith, J.D., 1989. Flow in meandering channels with natural topography. In: Ikeda, S., Parker, G. (Eds.), River Meandering. AGU Water Resources Monograph 12, Washington, D.C., pp. 69–102
Nelson, J.M., Bennett, J.P., Wiele, S., 2003. Flow and sediment transport modeling, chapter 18. In: Kondolph, G.M., Piegay, H. (Eds.), Tools in Fluvial Geomorphology. Wiley and Sons, Chichester, pp. 539–576.
O'Connor, J.E., Mangano, J.F., Anderson, S.W., Wallick, J.R., Jones, K.L., Keith, M.K., 2014. Geologic and physiographic controls on bed-material yield, transport, and channel morphology for alluvial and bedrock rivers, western Oregon. Geol. Soc. Am. Bull. 126 (3–4), 377–397.
Osmundson, D.B., Ryel, R.J., Lamarra, V.L., Pitlick, J., 2002. Flow-sediment-biota relations: implications for river regulation effects on native fish abundance. Ecol. Appl. 12, 1719–1739.
Parker, G., 1990. Surface-based bedload transport relation for gravel rivers. J. Hydraul. Res. 28, 417–436.
Paustian, S.J., Beschta, R.L., 1979. The suspended sediment regime of an oregon coast range streams. J. Am. Water Res. Assoc. 15 (1), 144–154.
Peckarsky, B.L., McIntosh, A.R., Horn, S.C., McHugh, K., Booker, D.J., Wilcox, A.C., Brown, W., Alvarez, M., 2014. Characterizing disturbance regimes of mountain streams. Freshwater. Science 33 (3), 716–730.
Peterson, C.G., Stevenson, R.J., 1992. Resistance and resilience of lotic algal communities - importance of disturbance timing and current. Ecology 73, 1445–1461.
Peterson, C.G., Weibel, A.C., Grimm, N.B., Fisher, S.G., 1994. Mechanisms of benthic algal recovery following spates - comparison of simulated and natural events. Oecologia 98 (3–4), 280–290.
Pitlick, J., Wilcock, P., 2013. Relations between streamflow, sediment transport, and aquatic habitat in regulated rivers, geomorphic processes and riverine habitat. Am. Geophys. Union 185–198.
Power, M.E., Stewart, A.J., 1987. Disturbance and recovery of an algal assemblage following flooding in an Oklahoma stream. Am. Midl. Nat. 117 (2), 333–345.
Reice, S.R., Wissmar, R.C., Naiman, R.J., 1990. Disturbance regimes, resilience, and recovery of animal communities and habitats in lotic ecosystems. Environ. Manag. 14, 647–659.
Resh, V., Brown, A., Covich, A., Gurtz, M., Li, H., Minshall, S., Reice, S., Sheldon, A., Wallace, B., Wissmar, R., 1988. The role of disturbance in stream ecology. J. N. Am. Benthol. Soc. 7, 433–455.
Roberts, B.J., Mulholland, P.J., Hill, W.R., 2007. Multiple scales of temporal variability in ecosystem metabolism rates: results from 2 years of continuous monitoring in a forested headwater stream. Ecosystems 10 (4), 588–606.
Rosenfeld, J.S., Hudson, J.J., 1997. Primary production, bacterial production, and invertebrate biomass in pools and riffles in southern Ontario streams. Archiv Fur Hydrobiologie 139 (3), 301–316.
Rosenfeld, J., Roff, J.C., 1991. Primary production and potential availability of autochthonous carbon in Southner Ontario streams. Hydrobiologia 224 (2), 99–109.
Schneck, F., Melo, A.S., 2012. Hydrological disturbance overrides the effect of substratum roughness on the resistance and resilience of stream benthic algae. Freshw. Biol. 57 (8), 1678–1688.
Segura, C., Pitlick, J., 2015. Coupling fluvial-hydraulic models to predict gravel transport in spatially variable flows. J. Geophys. Res. Earth Surf. 120:834–855. https://doi.org/10.1002/2014JF003302.
Segura, C., McCutchan, J.H., Lewis, W.M., Pitlick, J., 2011. The influence of channel bed disturbance on algal biomass in a Colorado mountain stream. Ecohydrology 4 (3), 411–421.
Sekar, R., Nandakumar, K., Venugopalan, V.P., Nair, K.V.K., Rao, V.N.R., 1999. Spatial variation in microalgal colonization on hard surfaces in a lentic freshwater environment. Biofouling 13 (3), 177–195.
Snell, M.A., Barker, P.A., Surridge, B.W.J., Large, A.R.G., Jonczyk, J., Benskin, C.M.H., Reaney, S., Perks, M.T., Owen, G.J., Cleasby, W., Deasy, C., Burke, S., Haygarth, P.M., 2014. High frequency variability of environmental drivers determining benthic community dynamics in headwater streams. Environ. Sci.: Processes Impacts 16 (7), 1629–1636.
Stanley, E.H., Powers, S.M., Lottig, N.R., 2010. The evolving legacy of disturbance in stream ecology: concepts, contributions, and coming challenges. J. N. Am. Benthol. Soc. 29 (1), 67–83.
Stevenson, R.J., 1990. Benthic algal community dynamics in a stream during and after a spate. J. N. Am. Benthol. Soc. 9 (3), 277–288.
Stewart, G., Anderson, R., Wohl, E., 2005. Two-dimensional modelling of habitat suitability as a function of discharge on two Colorado rivers. River Res. Appl. 21 (10), 1061–1074.
Townsend, S.A., Douglas, M.M., 2014. Benthic algal resilience to frequent wet-season storm flows in low-order streams in the Australian tropical savanna. Freshwater Sci. 33 (4), 1030–1042.
Townsend, S.A., Padovan, A.V., 2005. The seasonal accrual and loss of benthic algae (Spirogyra) in the Daly River, an oligotrophic river in tropical Australia. Mar. Freshw. Res. 56 (3), 317–327.
Uehlinger, U., 2000. Resistance and resilience of ecosystem metabolism in a flood-prone river system. Freshw. Biol. 45 (3), 319–332.
Uehlinger, U., 2006. Annual cycle and inter-annual variability of gross primary production and ecosystem respiration in a floodprone river during a 15-year period. Freshw. Biol. 51 (5), 938–950.
Uehlinger, U., Buhrer, H., Reichert, P., 1996. Periphyton dynamics in a floodprone prealpine river: evaluation of significant processes by modelling. Freshw. Biol. 36 (2), 249–263.
Uehlinger, U., Kawecka, B., Robinson, C.T., 2003. Effects of experimental floods on periphyton and stream metabolism below a high dam in the Swiss Alps (River Spol). Aquat. Sci. 65 (3), 199–209.
Warren, D.R., Collins, S.M., Purvis, E.M., Kaylor, M.J., Bechtold, H.A., 2017. Spatial variability in light yields colimitation of primary production by both light and nutrients in a forested stream ecosystem. Ecosystems 20 (1), 198–210.
Wolman, M.G., 1954. A method of sampling coarse river bed material. Trans. Am. Geophys. Union 35 (6), 951–956.

Please cite this article as: Katz, S.B., et al., The influence of channel bed disturbance on benthic Chlorophyll *a*: A high resolution perspective, Geomorphology (2017), https://doi.org/10.1016/j.geomorph.2017.11.010